Dalton Transactions

Accepted Manuscript

View Article Online
DOI: 10.1039/C6DT01468B

Structure characterization of non-crystalline complexes of copper salts with native cyclodextrins

Manuel I. Velasco,[a] Claudio R. Krapacher,[a] Rita Hoyos de Rossi,[a] Laura I. Rossi.[a*]

[a] Instituto de Investigaciones en Físico Química de Córdoba (INFIQC) - CONICET, Departamento de Química Orgánica, Facultad de Ciencias Químicas, Universidad Nacional de Córdoba, Ciudad Universitaria. X5000HUA Córdoba, Argentina.

ABSTRACT

The characterization of non crystalline complexes is particularly difficult when techniques like X-Ray diffraction or NMR cannot be used. We propose a simple procedure to characterize the physicochemical properties of amorphous new coordination compounds between cyclodextrins (CD) and Cu^{2+} salts, by means of the integration of the information provided by several techniques including elemental analysis, flame atomic absorption, TGA, UV-Vis Diffuse Reflectance, colorimetry, FT-IR and EPR. On the basis of these procedures, we suggest geometrical and structural approximations resulting in an octahedral or distorted octahedral geometry with diverse positions for the metallic centre. According to EPR spectrum, only one of the complexes may have rhombic symmetry. We also analyzed enthalpy-entropy compensation and isokinetic effect. In addition, general trends in thermal

* Corresponding autor.
[a] (INFIQC-CONICET) Departamento de Química Orgánica, Facultad de Ciencias Químicas, Universidad Nacional de Córdoba, Ciudad Universitaria. X5000HUA Córdoba, Argentina. Tel: +54-351-5353867. E-mail address: mvelasco@fcq.unc.edu.ar (Manuel I. Velasco); ckrapacher@fcq.unc.edu.ar (Claudio R. Krapacher); ritah@fcq.unc.edu.ar (Rita Hoyos de Rossi); lauraros@fcq.unc.edu.ar (Laura I. Rossi)*

View Article Online
DOI: 10.1039/C6DT01468B

stability, spectroscopic properties and inclusion in the cavity were analysed. This completes characterization methodology become essential for their future application as catalysts.

Keywords: copper complex, cyclodextrins, TGA, spectroscopy, FT-IR, EPR.

Chemical compounds used in this article

α-cyclodextrin (αCD) (PubChem CID: 444913); β-cyclodextrin(βCD)(PubChem CID: 444041); γ-cyclodextrin(γCD)(PubChem CID: 86575); copper (II) nitrate [$Cu(NO_3)_2$] (PubChem CID: 18616); copper (II) chloride ($CuCl_2$) (PubChem CID: 24014); copper (II) bromide ($CuBr_2$) (PubChem CID: 24611).

1. Introduction

Copper compounds play a key role in various scientific fields, such as organic synthesis,[1,2] catalysis,[3,4,5] materials design,[6,7,8] and biological processes.[9] They are also central for recovering Cu(II) from industrial waste, and carbohydrate polymers have been proposed for this purpose.[10,11] The structure elucidation of copper complexes greatly benefits all these areas, since detailed structural information is often essential for a fully understanding of the mechanisms involved.

On the other hand, in the last 50 years, cyclodextrins (CDs) have been widely used as hosts in the formation of several inclusion complexes with organic, organometallic[12,13] and, to a lesser extent, inorganic guests.[14,15,16] Most of the inclusion complexes has been studied using the classical techniques for solution-state or, when possible, X-Ray diffraction.[17,18] The metal based CD complexes subject was recently reviewed.[19] The majority of complexes reported in literature were prepared in basic solution;[20] but there are a few synthesized in deionized water without the addition of base[21] and one synthesized in toluene.[22]

View Article Online
DOI: 10.1039/C6DT01468B

We have previously reported the synthesis of transition metal salt-CD complexes in different organic solvents,[23] as well as their application as heterogeneous catalysts in sulfoxidation reactions.[24] The main advantage of the synthesis is its simplicity, quantitative yield and agreement with the aims of the Green Chemistry Principles.[25] On the other hand, it is important to remark that the complexes are very stable under normal laboratory conditions and can be stored without any special care. It is worth to note that for the oxidation of methylphenylsulfide, the complex βCD/$FeBr_3$ prepared in 1/1 ratio, was better catalyst than complexes prepared in other solvents which are formed with higher βCD/Fe ratio. Those complexes do not behave properly and the mixtures after reaction were very difficult to separate.[23] It is unfortunate that the physicochemical characterization of these compounds is quite complex since the most direct alternative for structural determination which is X-Ray diffraction study of monocristals cannot be used. The problem is that, in order to obtain a crystal appropriate for X-Ray structure determination, it is necessary to dissolve the species and then to get the crystals from the solution. This procedure may led to a crystalline complex but it does not warranty that the structure is the same as that of the complexes formed as we report here. Complexes are soluble in aqueous media or DMSO, and their main mechanism of dissolution is the solvation of both host and guest. This leads to the dissociation of the complex, therefore despite many efforts done during several years; the formation of a single crystal has not been achieved. Besides, even if a complex could crystallize from the solution, the competition between the guest and the solvent would not allow to ensure that the structure elucidated by X-Ray would be the same as that of the product obtained in dichloromethane; therefore, this information would not be useful. In previous studies,[23] it was observed that 24h after dissolution of the βCDFe complex in ethanol, at room temperature, βCD precipitated; this result indicated that the solvent could displace βCD from the coordinated sphere of metal.

View Article Online
DOI: 10.1039/C6DT01468B

In many studies of complexes between transition metal and carbohydrates and/or cyclodextrins, Nuclear Magnetic Resonance (NMR) has played an important role in the elucidation of their structure.[26,27] Generally, experiments involve the classical ^{1}H and ^{13}C nucleus, although some coordination compounds with organic substrates with heteroatoms have been analysed using ^{31}P, ^{15}N and ^{19}F signals.[28] Due to the paramagnetic characteristics of the Cu^{2+} salts that produce a fast relaxation of the surrounding nuclei; it usually results in broad line widths and poor spectral resolution, making interpretation very difficult,[29] if not impossible. Only few studies report on the structural elucidation of Cu^{2+} complexes whit carbohydrates;[30] they mostly consist on high molecular weight carbohydrates such as starch with low amounts of metal cation in solution. [6,27,31,32] As previously stated, such studies are not directly relevant to the complexes reported here due to their high metal content and results obtained in solution are not directly transferable to the complex used as a catalyst.

With the aim to determine the relationship between the catalytic activity and the structure of the complex it is desirable to thoroughly characterize the compound and establish the location of the metal in the complex, whether inside or outside the cavity, among other important structural information. Structural characterization is also very important for the quality control of the complexes if they are going to be used as catalysts.

In many instances, cyclodextrin inclusion complexes have been studied by comparison between the results of the analysis of the host and guest taken individually, with those of their physical mixture and the complex formed.[33] This procedure does not apply to our guests, since most of the transition metal salts are highly hygroscopic, and it is not possible to know whether the analysis is being performed on the starting salt, its hydrate, oxide or intermediate species. Moreover, in many cases, the hydration-decomposition process of the sample is

View Article Online
DOI: 10.1039/C6DT01468B

associated with the release of corrosive gases such as HBr which may damage the equipment used for the measurements.

Consequently, the characterization of these complexes should be done using techniques where the sample is in its powder state, does not undergo processing -or rather a minimum one- and does not alter the identity of the complex. Generally, these techniques provide incomplete information; therefore, we have developed a methodology which involves the analysis of the data in an integrated manner. The aim of this work was to characterize and analyze $CDCuX_2$ complexes using as many techniques as possible. In addition to these analyses, we calculated kinetic parameters of thermal studies and we elaborated a simple and reliable procedure to characterize the physicochemical properties of amorphous complexes obtained from native α, β or γCD, and copper II bromide, chloride or nitrate salts that may be of future importance for the use of these complexes as catalysts.

2. Experimental

2.1. Synthesis of metal complexes

All complexes were prepared in a way similar to that previously reported for $FeBr_3$.[23] 0.8 mmol of Cu^{2+} salt in 10mL of dichloromethane was stirred for 30 min; solid cyclodextrin was then added in 1:1 molar ratio. The heterogeneous mixture was stirred for 24 h, after which the solid was filtered, washed with extra solvent and dried under air. The recovered mass was within 97% and 100% of the total mass initially used. During complex formation we could observe organic solvent decolouration in contrast to colouration of the white CD powder.

2.2. Stoichiometry determination

View Article Online
DOI: 10.1039/C6DT01468B

Stoichiometry determination of the complex requires the combination of the data provided by the different analyses. From the data resulting from elemental analysis and flame atomic absorption, we could determine the percentages of C, H, O, N and Cu in the sample. Infinite molecular formulas may arise from these percentage values, so it is necessary to apply some constraints to these calculations, in order to lessen possibilities. The constraints were:

i: the only carbon source was cyclodextrin and the relations between C, H and O would remain fixed as in CD.

ii: the cation/anion ratio of the metal salt remains constant.

iii: the water amount only affects the values of H and O in a 2 to 1 ratio.

thus, a complex of βCD with CuX_2 will have the general formula:

$$A\left(C_{42}H_{70}O_{35}\right)\cdot B\left(CuX_2\right)\cdot D\left(H_2O\right)$$

Considering the molecular weight of the complex (MW), the % of each element will be determined as follows (eq 1-5):

$$\%C = \frac{42\cdot A\cdot 12.01}{MW}\times 100 \quad (1)$$

$$\%H = \frac{\left(70\cdot A + 2\cdot D\right)\cdot 1.01}{MW}\times 100 \quad (2)$$

$$\%O = \frac{\left(35\cdot A + D\right)\cdot 16.00}{MW}\times 100 \quad (3)$$

$$\%Cu = \frac{B\cdot 63.54}{MW}\times 100 \quad (4)$$

$$\%X = 100 - \left(\%C + \%H + \%O + \%M\right) \quad (5)$$

The percent compositions of theoretical complexes were calculated using A:B ratios 1:1, 1:2, 1:3, 2:1, 3:2, 2:3 for each one, different D value from 1 to 40 in 0.5 intervals were

View Article Online
DOI: 10.1039/C6DT01468B

used. This leads to 468 theoretical percent compositions which were compared with data obtained experimentally through a linear regression analysis in terms of the R^2 and slope, both as near to 1 as possible.

2.3. Elemental analysis

Measurements were performed on a combustion-gas chromatography Perkin Elmer 2400 Series II CHNS, calibrated with standard cystine sample (Perkin Elmer, 99.99%). All samples were analyzed in quintuplicate directly from solid complexes.

2.4. Flame atomic absorption

The measurements were made on a Perkin Elmer Mod. 3110 with air-acetylene flame. Sample digestion involved dissolving about 10 mg of complex with 2 mL of concentrated HNO_3 and 2 mL of concentrated HCl for 1 h. The solution was then completed to 5 mL with milliQ water.

2.5. Thermal gravimetric analysis

TGA analyses were performed on thermogravimetric analyzer equipment Hi-Res Modulated TGA 2950. Samples were measured from 25 °C to 500 °C with a rate of 10 °C/min directly from solid complexes. Derivative thermogravimetric analyses (DTGA) were calculated from experimental thermograms.

2.6. UV-Vis diffuse reflectance

For the analysis of the samples, BLACK-Comet StellarNet Inc spectrometer equipment was used with UV-VIS optical fibbers suitable for measuring diffuse reflectance and colorimetry. Spectra were acquired in the range of 200 to 800 nm (50000 to 12500 cm^{-1}).

View Article Online
DOI: 10.1039/C6DT01468B

Each sample was measured 10 times and data were averaged. The reflectance (R) data obtained were parameterized using the Kubelka-Munk equation[34] (eq 6) and the spectra were deconvoluted using PeakFit Software.

$$F(R) = \frac{(1-R)^2}{2R} \tag{6}$$

For colorimetric measurement, SpectraWiz® Spectroscopy Software was used, and CIELab parameters a, b and L were obtained with D65 illuminant, also averaging 10 measurements.[35] The CIELab has a large colour gamut and is considered the most accurate colour model; this colorimetric method was used as recommended by the Commission Internationale de l' Eclairage. The **a** axis extends from green (-**a**) to red (+**a**) and the **b** axis from blue (-**b**) to yellow (+**b**); lightness (**L**) axis is perpendicular to (**a**) and (**b**) plane with a value of 0 for black and 100 for white.

2.7. FT-IR

The spectra were taken on a Nicolet 5SC spectrophotometer using KBr pellets containing 1% of the sample. 40 spectra were acquired at a resolution of 2 cm^{-1}. For complexes with chloride anions, KCl was used instead of KBr to avoid ligand exchange with the matrix due to compression. In all cases background was corrected using a pellet of pure KBr or KCl. Processing was performed in OMNIC software by careful correction of the baseline, and the absorbance or transmittance values were normalized to the intensity of the signal at 2800 cm^{-1} (C-H). The main differences between the spectra of pure CD and the complex were in the regions of 3300-2900 cm^{-1}, corresponding to the stretching of primary and secondary OH and 1600-1680 cm^{-1} assigned to water molecules in the cavity of the CD. Less significant changes were observed in the signals at 1225-1240 cm^{-1} (CH bending and OH

View Article Online
DOI: 10.1039/C6DT01468B

in plane bending), 1080-1120 cm^{-1} (CO stretching of the secondary OH), 1035-1060 cm^{-1} (CO stretching of the primary OH) and the region of 920-960 cm^{-1} assigned to ring vibrations.[36]

It has been reported that a bathochromic shift in the maximum of the signal corresponding to the stretching of OH suggests that hydrogen bonds between CD molecules have weakened due to interactions with the host.[37] This analysis can be extended also to the signal at 1640cm^{-1}. The maximum of these signals was determined using the appropriate software function, and these values were subtracted from those of the native CD (eq 7). Only differences greater than 10 cm^{-1} were considered significant.[38]

$$\nu_{Complex} - \nu_{CD} = \Delta\nu \tag{7}$$

2.8. EPR

Powder EPR spectra were acquired at room temperature with a Bruker EMX-Plus spectrometer using 9.8 GHz (X-band), equipped with rectangular cavity and field modulation frequency of 100 kHz. (Department of Physics, FByCB-UNL). The EPR spectra were simulated by EasySpin using the core functions ‘Esfit’ and ‘Pepper’.

3. Results and discussion

It is important to note that during the synthetic process, only dichloromethane was used as an organic solvent, and no water was used, thus Cu salts could not be hydrolysed or denatured. Halocuprate species are known to be stable in non-aqueous media,[39,40] for example, acetonitrile or dichloromethane.[41]

In order to understand the results, it should be considered that the complexes are made up from cyclodextrin (macrocyclic oligosaccharide bearing glucosidic oxygen and primary and secondary OH groups) and Cu salt [$CuCl_2$, $CuBr_2$ or $Cu(NO_3)_2$]; therefore, coordination

View Article Online
DOI: 10.1039/C6DT01468B

between the macrocycle and the metallic centre is expected. Besides the counterions (Br^-, Cl^- and NO_3^-) may also form part of the coordination sphere of the metal. This fact should be observed or inferred from the studies realized.

In order to get information about the physical chemical properties and structure of the complexes, results from different techniques were analysed in an integrated way as it will be described below. As an example, a comprehensive description of the procedure is shown for αCD and $CuBr_2$ complex (αCDCuBr$_2$). In general, a similar analysis can be extended to the other complexes discussed in this paper. (See Supplementary Data, Figures 1S-16S and Table 1S- 2S).

From the results of elemental analysis (EA) and flame atomic absorption, it was determined that the molecular formula for αCDCuBr$_2$ is $D H_2O \cdot (C_{36}H_{60}O_{30}) \cdot (CuBr_2)$ so there is a 1:1 relationship between α-CD and $CuBr_2$. The value of D calculated from EA data is 6 while TGA analysis yield a value of 9.4 (see Supplementary Data, Table 1S for native CDs and other complexes).

3.1. Thermogravimetric analysis

The thermal analysis (TGA and DTGA) of αCD are in good agreement with data reported in the literature[42] but they are significantly different with those of the complex (see Figure 1). In the DTGA plots the two peaks at 50 and 71 ºC which are attributed to the release of hydration water molecules[43] (hwm) appear in both compounds but the complex has an additional peak at 144 ºC, that can be attributed to coordinated water molecules. The reason to believe that this mass release correspond to coordinated water molecules (cwm) is that all the complexes studied have similar signals in the temperature range 144-159ºC (see Table 1 and Figures 1S, 3S, 5S, 7S, 9S, 11S, 13S, 15S in the Supplementary Data). Whereas there is no regularity in the behaviour of the different complexes above this temperature (see Table 1).

View Article Online
DOI: 10.1039/C6DT01468B

The fact that the elimination of some water molecules takes place at high temperature, has been considered as evidence that they are coordinated to the metal centre.[9]

The decomposition kinetics of the complexes is also very different to that of native CD; while the native CD shows only one clear thermal transition at 307°C, the degradation of the macrocycle in αCDCuBr_2 takes place in several steps. The smaller fragments generated from initial carbohydrates, are coordinated to the metallic centre and therefore are eliminated at different temperatures.[44] Similar behaviour was observed in all complexes (see Supplementary Data, Figures 1S, 3S, 5S, 7S, 9S, 11S, 13S, 15S). Only βCDCuBr_2 complex showed degradation of the macrocycle immediately after 146 ºC (See Figure 13S), probably HBr loss occurs and it catalyzes the cleavage of CD.

The thermal stability of the complexes can be discussed in terms of different parameters, i.e., decomposition temperature of 50% of the initial mass (T_d50%), the initial temperature of macrocyclic decomposition step (T_{dec}) and the temperature value of the transitions in the DTGA. As shown in Table 1, the T_d50% value of the complexes is in all cases lower than that of the native CD and the initiation of the decomposition event takes place almost immediately after the last process of coordinated water loss. This effect was observed in all complexes. Hence, it can be concluded that the presence of the inorganic salt accelerates the thermal decomposition of the macrocycle; this effect is not only dependent on the metal ion but also it depends on the counterion.

Figure 1: TGA and DTGA of αCDCuBr_2 complex (solid lines) and αCD (dotted line)

View Article Online
DOI: 10.1039/C6DT01468B

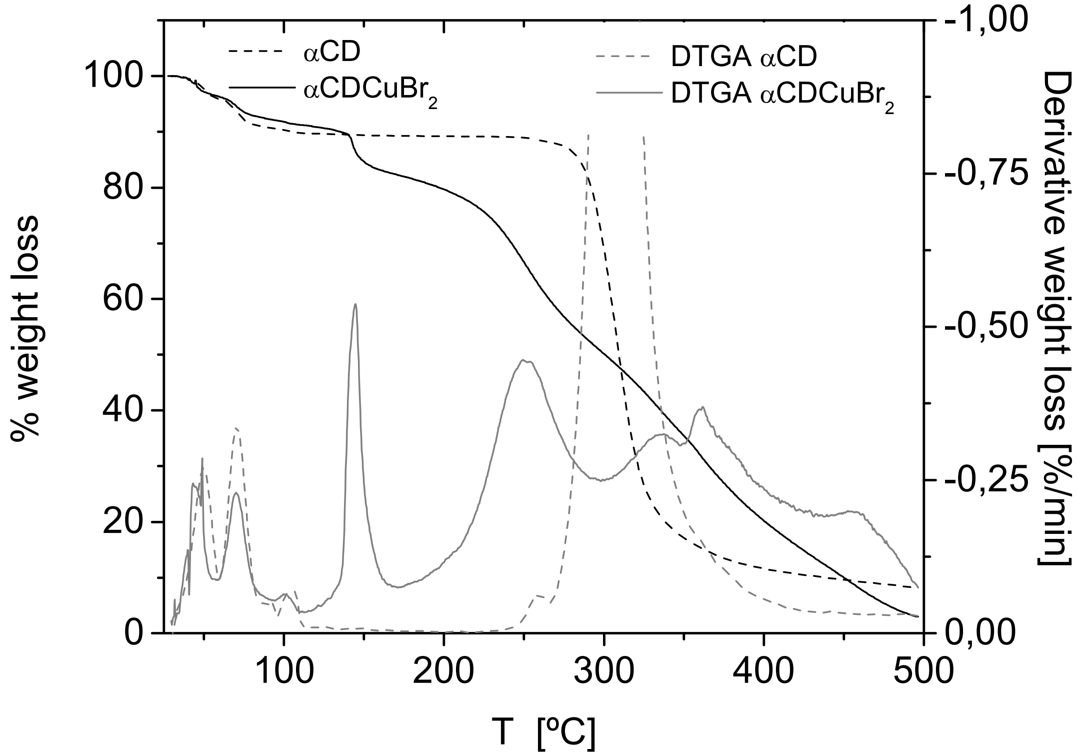

Analysis of the remaining mass (%m_r) can also give a clue about the complexes structure (see Table1). All αCD complexes gave %m_r lower than the native CD whereas in all the other complexes with β or γCD except for γCDCu$(NO_3)_2$, the remaining mass is higher than in the corresponding CD; these results might indicate that in complexes with β or γCD the coordination of the oxygens of the host with the metal is stronger than in case of αCD. It is to be noted that the number of coordinated water in αCD complexes is higher than in all the others except for γCDCuBr_2; i.e. the metal is mainly coordinated to water in αCD complexes and to cyclodextrin oxygens in β or γCD complexes.

Table 1: Thermal analysis results.

Native or Complex CDs	**T_{cwm}[a] (ºC) hwm[b] ; cwm[c]**	**T_{dec}[d] (ºC)**	**T_d50%[e] (ºC)**	**%m_r[f]**

View Article Online
DOI: 10.1039/C6DT01468B

αCD	-- 5.8 ; --	250	309	8.18
$\alpha CDCuCl_2$	159 3.3 ; 4.2	210	300	2.94
$\alpha CDCuBr_2$	144 5.7 ; 3.7	180	300	2.99
$\alpha CDCu(NO_3)_2$	153 2.0 ; 3.8	220	300	5.10
βCD	-- 7.4 , --	270	328	7.65
$\beta CDCuCl_2$	149 6.8 ; 1.5	220	300	9.74
$\beta CDCuBr_2$	146 6.3 ; 1	138	324	27.03
$\beta CDCu(NO_3)_2$	159 8.2 ; 2.6	220	286	7.90
γCD	-- 6.0 ; --	270	312	8.48
$\gamma CDCuCl_2$	148 7.5 ; 1.1	190	299	16.00
$\gamma CDCuBr_2$	149 4.6 ; 6.3	200	308	16.54
$\gamma CDCu(NO_3)_2$	158 4.0 ; 1.6	200	295	0.21

[a] T_{cwm}: Temperature of mass loss corresponding to coordinated water molecules.

[b] hwm = number of hydration water molecules

[c] cwm = number of coordinated water molecules

[d] T_{dec}: Initial temperature of macrocyclic decomposition step.

[e] T_d50%: Decomposition temperature of 50% of the initial mass.

View Article Online
DOI: 10.1039/C6DT01468B

[f] $\%m_r$: Percentage of remaining mass.

It is also interesting to compare the effect of the counterions on the $\%m_r$. While for αCD complexes, αCDCu$(NO_3)_2$ is the one among the three which gave the higher $\%m_r$ value, in the β and γCD complexes the nitrate derivative gave the lower mass recover. In fact, the γCDCu$(NO_3)_2$ complex decomposes almost completely ($\%m_r$ is 0.21). Since NO_3^- is a highly oxidant agent, these results might indicate that in the later complex the Cu ion is mainly coordinated to the CD. Therefore, the NO_3^- ion is able to act as oxidant in γCDCu$(NO_3)_2$ while in the αCD complex the metal is mainly coordinated to the NO_3^- anion.[45] It is known that the volatility of metal-organic complexes can be correlated with their structures considering at least two factors: the absence/presence of intermolecular hydrogen bonding and intermolecular Van der Waals interactions; so, the conformation of complexes probably determines whether a complex sublimes or not,[46] as it has been reported for β-CD/CoI_2 complex.[47]

The thermal behaviour of the complexes reported here was also different to that of other complexes found in the literature.[14] These discrepance may be attributed to dissimilar synthetic processes that lead to compounds with different structures.[21]

3.2. Thermodynamic relationship

Coats-Redfern has developed a method to calculate kinetic parameters from thermogravimetric data.[48] Dynamic TG techniques have been used in the dehydration study of bentonite,[49,50] magnesita[51] and metal chelates.[52] In this work, the temperature range where the main thermal processes of native CDs occurs (40-350)ºC was divided in two sectors: loss hydration water molecules (40-110)ºC and macrocyclic structure decomposition (200-350)ºC; for complexes, it was necessary to include the (110-200)ºC range, on the basis of the obtained termograms.

View Article Online
DOI: 10.1039/C6DT01468B

The activation energy (E*) was calculated from the slope of a plot of the left hand side of eq. 8 *vs* 1/T:[53]

$$\log\left[\frac{\log[m_f/(m_f-m)]}{T^2}\right] = \log\left[\frac{AR}{\theta E^*}\left(1-\frac{2RT}{E^*}\right)\right] - \frac{E^*}{2.303RT} \quad (8)$$

In this equation, m_f is the mass loss at the completion of the heating process, m is the mass loss up to the temperature T (K) (this temperature corresponds to DTGA maximum), A is the pre-exponential factor, R is the universal gas constant, θ is the heating rate ($K\cdot min^{-1}$), E^* is the activation energy ($kJ\cdot mol^{-1}$). Enthalpy (ΔH^*), entropy (ΔS^*) and free energy (ΔG^*) of activation were calculated using eq. 9-11 where h and k are the Plank and Boltzman constants, respectively:

$$\Delta H^* = E^* - RT \quad (9)$$

$$\Delta S^* = 2.303[log(Ah/kT)]\,R \quad (10)$$

$$\Delta G^* = \Delta H^* - T\Delta S^* \quad (11)$$

The data are shown in Table 2S, Table 3S and Figure 2.

The results showed different thermal processes depending on the compound studied; in each temperature range, more than one process of mass loss was observed (see Table 2S for individual values). In most cases, the complexes present lower E* values than those of native CDs at all temperature ranges (see Figure 2). Moreover, αCD complexes have a E* for the total process [(313-623)K] larger than that of other complexes presented in this paper; in this case, the first process (the loss of water molecules is associated to this step [(313-383)K]) was the main contributor to the total activation energy. All complexes showed different thermal decomposition pattern in a temperature range [(383-473)K] a region where native CDs do not present any thermal processes. It is worth to note that E* of $\beta CDCuBr_2$ was the highest value of all the compounds in this temperature range and that this complex had no other important thermal process at higher temperatures, in addition to have the highest remaining mass value (see Table 3s and Figure 13S). In the temperature range [(473-623)K] γCD complexes

View Article Online
DOI: 10.1039/C6DT01468B

exhibited the highest E* value, decomposition of macrocyclic structure is occurring at these temperatures.[42]

In summary, $CDCuX_2$ complexes showed different responses to thermogravimetric analysis between them and with native CDs as well. The temperature behavior of native CDs is different from that of their metal complexes and in all cases the stability of the macrocycle decreases in the complex.

Figure 2: Activation energies for the thermal decomposition of native CDs and their complexes.

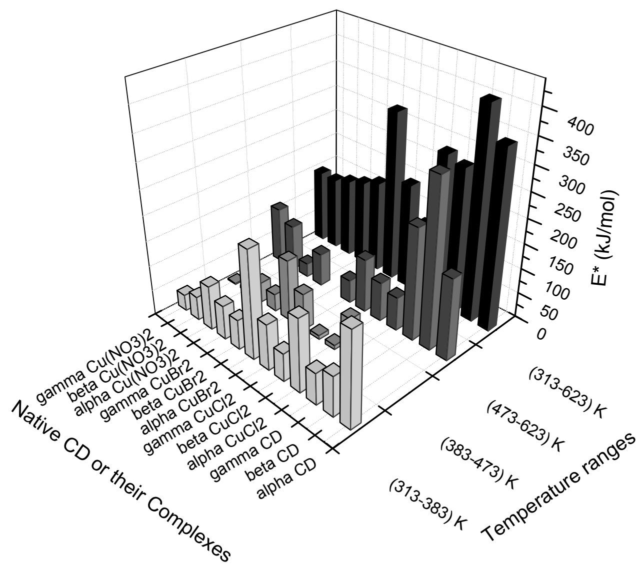

Enthalpy-entropy compensation and isokinetic effects were also analyzed; they are often called extra-thermodynamic relationships. After evaluating all thermal processes, we found a very good correlation between *Log A* and *E** only for the first mass loss process (water loss)[54] (Figure 3 and Table 2S). This fact may indicate that the first water releasing process is similar in all complexes and native CDs. Therefore, it should be related to water molecules which are not influenced by the presence of the salt. On the other hand, the other observed mass release phenomenons are not correlated; therefore they might be related to different interactions of the host with the guest.

View Article Online
DOI: 10.1039/C6DT01468B

Although the isokinetic effect was observed when the complexes were compared, the data for the native CDs do no cross the isokinetic point, as shown in Figure 4.[55] This fact could indicate that macrocycles structure were affected by the coordination of different Cu salts and the water molecules which are not coordinated to the metallic centre, were interacting in a similar way in all the complexes but different than in native CDs.[54]

Figure 3: Enthalpy-entropy compensation effect on the first process of mass loss in thermogravimetric studies.

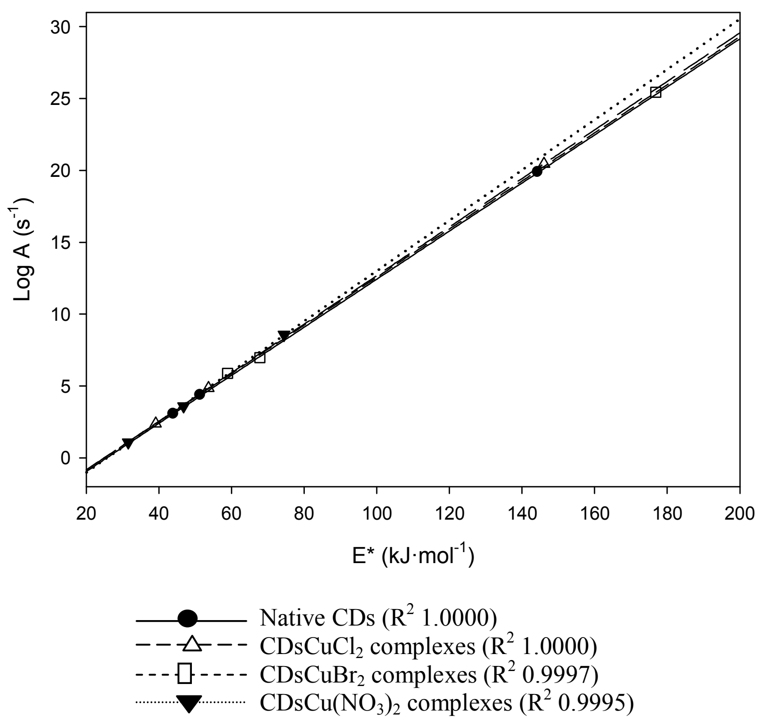

The results discussed previously indicate that the thermal behaviour of CDs and Cu salts complexes is strongly dependent on the counterion of the salt (Cl^- or Br^- or NO_3^-). Also, this is an evidence that counterions are in the first coordination sphere of the metal, playing an important role in the thermal decomposition of cyclodextrin complexes.

Besides, the fact that there is no isokinetic relationship between the mass loss processes taking place in the (383-623)K temperature range is considered an indicator that the

View Article Online
DOI: 10.1039/C6DT01468B

counterion of the metal takes part in the decomposition process probably inducing different mechanisms.

Figure 4: Isokinetic effect for the first mass loss process in thermogravimetric studies.

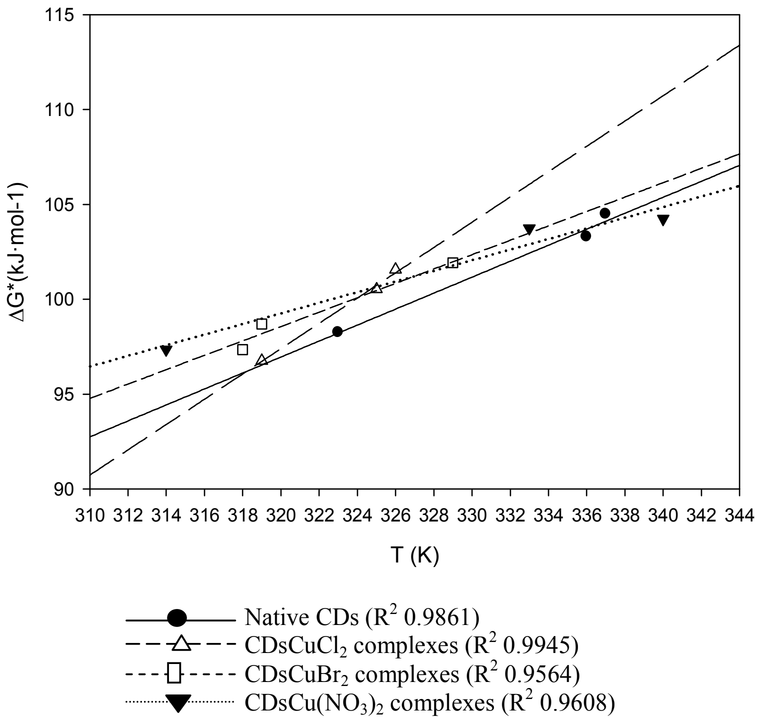

3.3. UV-vis diffuse reflectance

The difference in energy generated by the split of the *d* orbital into high and low energy orbitals, when ligands attach to a transition metal to form a coordination complex is called Δ_0 and it is a characteristic of both ligand and metal.[56] From UV-vis diffuse reflectance measurements, Δ_0 values, ligand-to-metal charge transfer (LMCT) and Jahn-Teller effect were analyzed.

Since Cu^{2+} has a d^9 configuration, only one transition should be expected in the Uv-Vis of the complex.[57] However, the distortion of the octahedron leads to other bands due to Jahn-Teller effect.[58] As these two bands are close in wavenumber values, the deconvolution of

View Article Online
DOI: 10.1039/C6DT01468B

the spectra with two Gaussians is necessary. Figure 4 exhibits the UV-Vis diffuse reflectance of the $\alpha CDCuBr_2$ powder as well as the bands resulting from the deconvolution of the spectra.

Figure 5: UV-Vis Diffuse Reflectance (DR) of $\alpha CDCuBr_2$. Dashed lines show the deconvolution of the bands (the maximum values are listed in Table 3).

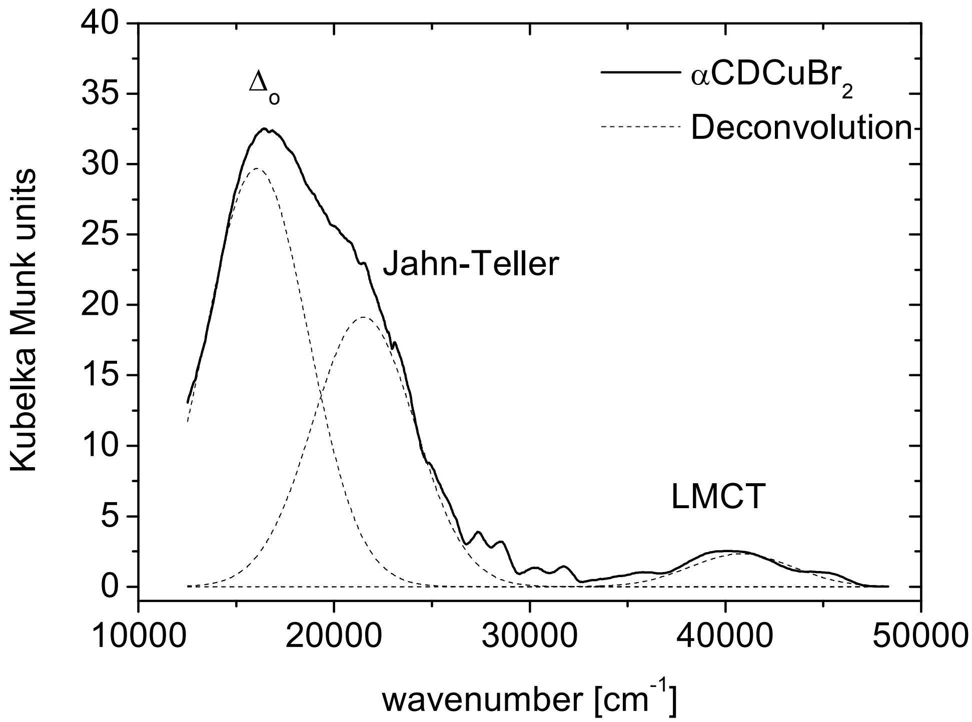

A value of Δ_o=16058 cm^{-1} is determined from the maximum of the highest intensity signal, consistent with an octahedral geometry.[57] The band at 21499 cm^{-1} is assigned to Jahn-Teller effect, and the band at 40802 cm^{-1} is assigned to a ligand-to-metal charge transfer (LMCT) transition.[58] This band is observed when the interaction between the host and the guest orbitals allows the transition (see also spectra of other complexes, Figures 2S, 4S, 6S, 8S, 10S, 12S, 14S, 16S and Table 3).

Since the only coordinating atoms in CDs are the oxygens, located in the cavity (glycosidic oxygens) and at the rim (primary or secondary OH groups), it is not possible to

View Article Online
DOI: 10.1039/C6DT01468B

determine a preferred position for the metal centre. However, it may be assumed that a higher orbital overlap is most favored as the guest is more included, since its mobility is constrained in a confined space and the interaction maybe more efficient.[59]

Figure 6: Schematic representation of different coordination possibilities for a Cu (II) metal centre with the same ligands in its first coordination sphere but in different arrays. [Schematic representation of possible isomers (no scale)]

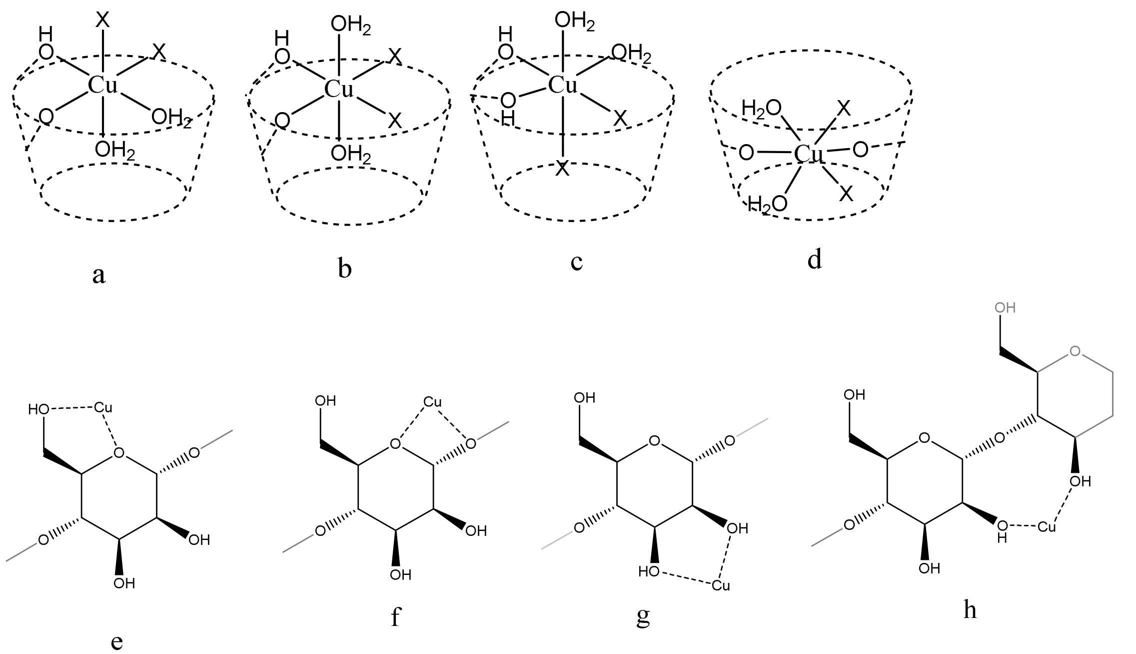

It should be noted that bands in the UV-Vis are broad suggesting that several isomers of the complex may be present in the powder. This is possible since more than one geometry would be allowed for a big ligand with multiple coordinating atoms such as cyclodextrin. Even with identical stoichiometry, three different ligands (halide, oxygen from water molecules, oxygen form CD) may be involved in the coordination process and differences in the coordination position (equatorial, axial or both) render Cu^{2+} atoms with different environments, what may cause a broadening in the UV-Vis bands. For illustrative proposes, Figure 6 shows some of the coordination possibilities for a general complex of $CDCuX_2(H_2O)_n$. For the same position of the metal atom, structures (a) to (c) show different

View Article Online
DOI: 10.1039/C6DT01468B

coordination possibilities, where axial position may be occupied by different ligands (a and c) or the same (b); the counterion can be in equatorial position (b) or in a combination of equatorial-axial inside or outside the cavity (a and c); (d) represent a complex were the Cu ion is bonded to two glycosidic oxygens and therefore implies that the Cu^{2+} is deeply included in the cavity. Schemes from (e) to (h) show some of the possible coordination for Cu^{2+} with the oxygen atoms of cyclodextrins, where only one glucose unit may be involved (e to g) or metal centre could bind two different ones (h); the coordination may involve primary OH (e); secondary OH (g), glycosidic O (f) or combination of these.

Table 3: Spectroscopic data of the complexes

Complex	Δ_0 (cm^{-1})	Jahn-Teller band (cm^{-1})	LMCT band(cm^{-1}) ; area (a.u.)	Color (CIE L*a*b*)		
				L	a	b
$\alpha CDCuCl_2$	18464	26659	---	96,09	-6,90	4,72
$\beta CDCuCl_2$	19325	27120	---	93.28	-9.97	6.78
$\gamma CDCuCl_2$	18570	26797	---	94.39	-20.09	24.24
$\alpha CDCuBr_2$	16058	21499	40802; 15,216.16	82.80	-1.98	19.44
$\beta CDCuBr_2$	13204	19317	40738; 11,013.44	39.95	-2.03	15.85
$\gamma CDCuBr_2$	14431	20658	40976; 68,677.15	96.09	-1.95	14.92
$\alpha CDCu(NO_3)_2$	1766.6	23495	---	83.19	-11.17	-1.49
$\beta CDCu(NO_3)_2$	20335	26125	---	80.03	-17.62	-9.72
$\gamma CDCu(NO_3)_2$	19823	27456	39895; 62,179.51	101.25	-4.03	2.34

From data in Table 3, it can be inferred that all complexes show a distorted octahedral geometry since the Jahn-Teller band is always present. In addition, all complexes with $CuBr_2$ and $\gamma CDCu(NO_3)_2$ show bands assignable to ligand-to-metal charge transfer (LMCT) transitions, but γCD complexes show a considerable value of area, indicating that several isomers of these complexes may be present in the powder.

View Article Online
DOI: 10.1039/C6DT01468B

Comparing the Δ_o values obtained for complexes of βCD and γCD with the different salts, it follows that the sequence observed is that predicted by the spectrochemical series:[60]

$$H_2O > {}^{-}OH > NO_3^- > Cl^- > Br^-$$

Remarkably, values arising from αCD, show a different trend $Cl^- > NO_3^- > Br^-$ suggesting that the smaller size of the macrocycle has a high effect on the coordination sphere of the Cu^{2+}.

The colorimetric measurements of different metallic compounds are frequently used mainly in scientific fields such as earth science,[61] food,[62] gemology[63] among others; however, the technique is seldom used to characterize organometallic compounds. The CIE L*a*b* parameters have been used in the characterization of inorganic lanthanide-iron-based oxide pigments and ceramic glazes;[64] to monitor oxidation in raw meat;[65] to find relationships between chemical and appearance data of grape seeds;[66] or to track bioactive compounds in foods.[67]

Figure 7: a* and b* parameters of the CIELab space of the different complexes.

View Article Online
DOI: 10.1039/C6DT01468B

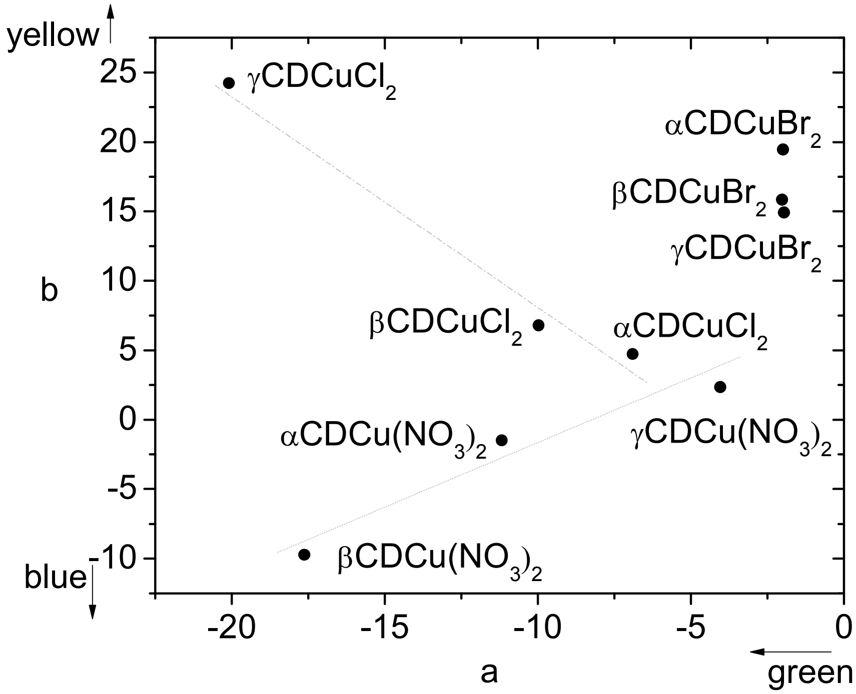

Table 3 displays the colorimetric data of the complexes, and Figure 7 shows the a* b* chromaticity diagram of the CIELAB color space. The positive direction of the horizontal axis indicates a red component; the negative direction indicates a green component. The positive direction of the vertical axis indicates a yellow component while the negative indicates a blue one. The absolute value of the distance from the origin of coordinates to the colorimetric value indicates the chromaticity that expresses the intensity of the colour, and the greater the distance, the higher the chromaticity (Figure 8).

Figure 8: Chromaticity value of all the synthesized compounds.

View Article Online
DOI: 10.1039/C6DT01468B

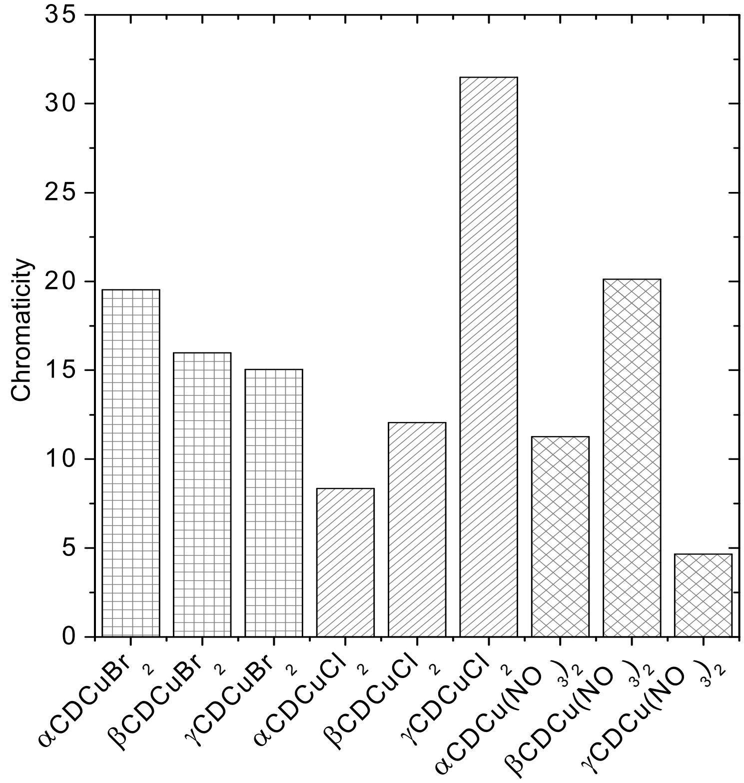

Although some tendencies may be outlined, the analysis of the data shows that colorimetric values are highly dependent on the counterion and the CD. The differences in the L a* and b* parameters show that the colorimetric values can be used as a fingerprint for these family of compounds, allowing the identification of each one by a simple procedure. It is noticeable that $\gamma CDCuCl_2$ is the complex that presents the higher absolute values of the CIELab parameters.

3.4. IR spectroscopy

In order to get more information about the structure of the complexes, we analysed the IR spectra. As indicated in the experimental section, we have chosen to discuss the regions of 3300-2900 cm^{-1}, corresponding to primary and secondary OH of the CD (OH_{rim}) and 1600-1680 cm^{-1} assigned to water molecules in the cavity of the CD (H_2O_{cavity}).

View Article Online
DOI: 10.1039/C6DT01468B

If the differences in FT-IR spectra are considered (Figure 9) it may be observed that the two signals under analysis are significantly modified but with different relative magnitude. Differences in the signal of H_2O from the cavity evidence that the metal salt presents a certain degree of inclusion; yet, it also interacts with the OH at the rims of the CD, altering the formation of inter and/or intra molecular H bond.

The behaviour of β$CDCuBr_2$ complex is remarkable because it shows an important change in the signal corresponding to the water included in the cavity while the shift in the OH signals is significantly small, even outside experimental error. Besides this is the only complex where the change in the H_2O_{cavity} signal is larger than that in the OH_{rim} signal. This may indicate that the metal is deeply included in the cavity and there is not much interaction with the OH groups located at the rim of the cavity. For α$CDCuBr_2$, α$CDCu(NO_3)_2$ and β$CDCuCl_2$ complexes, there are also changes in the signal assigned to included water but the effect on rim OH signals was more important. The major change for the OH_{rim} vibration is observed for β$CDCuCl_2$ complex; it should also be noted that α$CDCu(NO_3)_2$ is the complex wich have significant changes in both signals analyzed. On the other hand, in all γCD complexes, the H_2O_{cavity} signal is only slightly affected.

Figure 9: Differences in the FT-IR bands analysed for all the synthesized compounds.

View Article Online
DOI: 10.1039/C6DT01468B

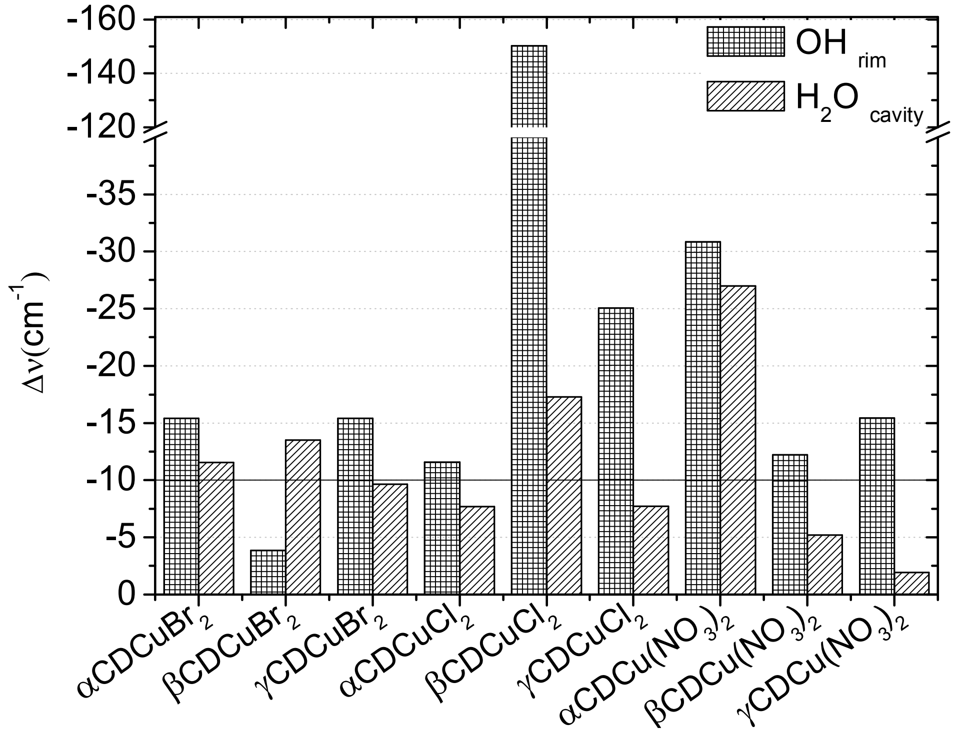

3.5. EPR spectroscopy

EPR spectroscopy is a good method for elucidating the structure of copper (II) complexes in various physical states, for example, liquid (or solution) and solid (powder, crystal or frozen solution). Usually, the ligands of Cu (II) are located in a distorted octahedral environment. The Cu^{2+} ion and four ligands are included in the same plane and the other two ligands are perpendicular to the plane and are located on a straight line including the metallic ion.[68] In order to get more information about the structure of the complexes, we analysed the EPR spectra. The g factors and others parameters are summarized in Table 4.

The averaged g-values (g_{av}) are calculated by expression $g_{av}= (g_{\parallel} +2g_{\perp})/3$ that relates the anisotropic parameters of g-factor.[69] Also, the g values are related by the expression $G = (g_{\parallel}-2)/(g_{\perp}-2)$; if $G > 4$ then the local tetragonal axes are aligned parallel or only slightly misaligned.[70] The values obtained are consistent with elongated tetragonal-octahedral

View Article Online
DOI: 10.1039/C6DT01468B

stereochemistry in all complexes except γCDCuCl$_2$ that would present rhombic symmetry because $g_x \neq g_y \neq g_z$, this is in agree with differences observed in CIELab parameters.

Table 4: Electron Paramagnetic Resonance spectra data of the complexes

Complex	***g* factors**						***G***[a]	***A***$_{\|\|}$**(G)** ($A_{\|\|}$(G))[c]	***Symmetry/Geometry***
(number in Fig.17S)	$g_\perp$ ($g_\perp$)[c]	$g_{\|\|}$ ($g_{\|\|}$)[c]	g_{av}[b]	g_z (g_z)[c]	g_y (g_y)[c]	g_x (g_x)[c]			
αCDCuCl$_2$ (1)	2.075 (2.0695)	2.380 (2.378)	2.177				5.067	115 (132.73)	axial/elongated octahedral
βCDCuCl$_2$ (2)	2.060 (2.0625)	2.310 (2.308)	2.143				5.167	140 (157.72)	axial/elongated octahedral
γCDCuCl$_2$				2.240 (2.242)	2.180 (2.176)	2.040 (2.043)			rhombic/distorted octahedral
αCDCuBr$_2$ (3)	2.050 (2.0458)	2.372 (2.370)	2.157				7.44	112 (129.88)	axial/elongated octahedral
βCDCuBr$_2$ (4)	2.090 (2.0847)	2.400 (2.398)	2.193				4.444	104 (121.67)	axial/elongated octahedral
γCDCuBr$_2$ (5)	2.085 (2.0928)	2.400 (2.398)	2.19				4.706	114 (121.67)	axial/elongated octahedral
αCDCu(NO$_3$)$_2$ (6)	2.085 (2.0836)	2.400 (2.398)	2.19				4.706	124 (141.65)	axial/elongated octahedral
βCDCu(NO$_3$)$_2$ (7)	2.062 (2.0661)	2.360 (2.362)	2.161				5.806	138 (146.65)	axial/elongated octahedral
γCDCu(NO$_3$)$_2$ (8)	2.085 (2.0799)	2.400 (2.398)	2.19				4.706	118 (146.65)	axial/elongated octahedral

[a] $G = (g_{||}-2)/(g_\perp-2)$

[b] $g_{av} = (g_{||} + 2g_\perp)/3$

[c] The spectra were simulated by EasySpin.

Axial symmetry of the complexes and the trend in g values $g_{||} > g_\perp > g_e$ (g-factor of free electron is $g_e = 2.0023$) suggested that the unpaired electron in the Cu^{2+} ion is in the $d_{x^2-y^2}$ orbital.[71] The correlation between hyperfine splitting ($A_{||}$) *versus* $g_{||}$, called Peisach-Blumberg diagram,[72] was consistent with the coordination by four oxygen atoms, Figure 17S. Experimental and simulated EPR spectra of αCDCuCl$_2$ and γCDCuCl$_2$ are shown in Figures 18S and 19S respectively.

In order to gain a better understanding of the possible applications of these compounds as catalysts, thermal stability must be considered. Reports in literature show that thermal stabilities of complexes depend strongly on the nature of both anionic and neutral ligands in

View Article Online
DOI: 10.1039/C6DT01468B

the Cu(II) coordination sphere.[73] Comparing the values of $T_d50\%$, it can be concluded that the presence of a metallic salt destabilizes the macrocycle. However, αCD is equally destabilized by any of the salt, since T50% value shows the smallest difference, suggesting that the size of the macrocycle is mandatory in the degradation process of these organometallic complexes. For βCD and γCD the thermal stability of the complex is mainly related to the chemical nature of the counterion. The stability trend is

$$Br^{-} > Cl^{-} > NO_3^{-}$$

This may be explained in terms of the thermal degradation of the metallic compound. During the heating process, nitrates decompose releasing different nitrogen oxidizing agents[74] that could favour decomposition of the macrocycle at temperatures lower than those normally required.

Although $T_d50\%$ is frequently used to compare the thermal stability of solid compounds in the case of the complexes reports here, these values are not useful since very small differences between $T_d50\%$ can be found for the complexes and the native CD. On the other hand, by analyzing DTGA curves it is evident that decomposition starts at a lower temperature in the complexes but the fragments remain coordinated with the metal and are slowly liberated. This proves that even though $T_d50\%$ values are close to the native CD, the presence of a metallic salt thermally destabilizes the carbohydrate.

Moreover, the percentage of remaining mass is an evidence of effect of salt coordination because it is high (27 %) in $\beta CDCuBr_2$ decomposition or low (0.21 %) in $\gamma CDCu(NO_3)_2$. These differences are a consequence of the type of interaction of the metal with the CD which not only depends on the size of the host but also on the associated counterion.

View Article Online
DOI: 10.1039/C6DT01468B

The analysis of kinetic parameters obtained from thermogravimetric analysis indicated that the only process that had similar behaviour in all complexes is the one corresponding to the first release of water molecules. All the results indicate that the structure of complexes is determined not only for the metal coordination with cyclodextrin but also for the counterions coordination to the metal.

4. Conclusion

It was determined that $CuBr_2$, $CuCl_2$ and $Cu(NO_3)_2$ form stable complexes with α, β and γCD. The procedure for the preparation is simple and yield complexes with 1:1 stoichiometry containing also water molecules. The reproducibility in the structure of the complexes obtained in several repetitive synthesis was determined after comparison of their TGA analysis, UV-Vis and IR spectra.

Through the integration of analytical data obtained by several techniques, it is possible to determine the stoichiometry and get an idea about the predominant interactions and some structural information of the different $CDCuX_2$ complexes. It is possible to standardize a method for the study of metal complexes using TGA, UV-Vis and FT-IR when NMR or single crystals X-ray diffraction analyses can not be applied due to the nature of the analyzed sample. Through EPR and reflectance measurements it was shown that the complexes have octahedral coordination geometry with varying degrees of distortion (*g*-factors and Jahn-Teller effect). This characterization methodology and studies to understand interactions between natural macrocyclics, metallic centre and counterions become essential in terms of their future applications as catalysts.

Acknowledgments

View Article Online
DOI: 10.1039/C6DT01468B

R.H.R and L.I.R are researchers from CONICET. M.I.V. and C.R.K. are grateful recipients of a fellowship from CONICET. C.RK. has had equal contribution with first author. Helpful discussions with Dr. Fagalde (INQUINOA) and Dr. Granados (INFIQC) are gratefully acknowledged. This research was partially supported by Consejo Nacional de Investigaciones Científicas y Técnicas (CONICET) (PIP 112-201101-00263), Agencia Nacional de Promoción Científica y Técnica (FONCYT) (PICT 2008-0180), Secretaría de Ciencia y Técnica (SeCyT) of Universidad Nacional de Córdoba (UNC) (SECyT Nº1565/14), Ministerio de Ciencia y Tecnología de Córdoba (MINCyT) (PID 2009-2011), Argentina.

References

1 A.V. Gulevich, A.S. Dudnik, N. Chernyak and V. Gevorgyan. *Chem. Rev.*, 2013, **113**, 3084-3213.

2 M.A. Thorseth, C.E. Tornow, E.C.M. Tse and A.A. Gewirth. *Coord. Chem. Rev.*, 2013, **257**, 130-139.

3 I. Jlalia, F. Gallier, N. Brodie-Linder, J. Uzie, J. Augé and N. Lubin-Germain. *J. Mol. Catal. A: Chem.*, 2014, **393**, 56-61.

4 C. Sambiagio, S.P. Marsden, A.J. Blacker and P.C. McGowan. *Chem. Soc. Rev.*, 2014, **43**, 3525-3550.

5 P. Tirino, R. Laurino, G. Maglio, M. Malinconico, G. Gomez d'Ayala and P. Laurienzo. *Carbohydr. Polym.*, 2014, **112**, 736-745.

6 A. Malik, S. Parveen, T. Ahamad, S.M. Alshehri, P.K. Singh and N. Nishat. *Bioinorg. Chem. Appl.*, 2010, **2010**, 1-8.

7 C. Ragupathi, J.J. Vijaya, L.J Kennedy and M. Bououdina. *Mat. Sci. Semicond. Process*, 2014, **24**, 146-156.

8 X. Zhang, Z. Chi, Y. Zhang, S. Liu and J. Xu. *J. Mat. Chem.C.*, 2013, **1**, 3376-3390.

9 S.E. Castillo-Blum and N. Barba-Behrens. *Coord. Chem. Rev.*, 2000, **196**, 3-30.

10 F-L. Mi, S-J Wu and F-M Lin. *Inter. J. Biol. Macromol.*, 2015, **72**, 136-144.

11 W. Ciesielski, C. Lii, M-T. Yen and P. Tomasik. *Carbohyd. Polym.*, 2003, **51**, 47-56.

View Article Online
DOI: 10.1039/C6DT01468B

12 N.M. Milović, J.D. Badjić and N.M. Kostić. *J. Am. Chem. Soc.*, 2004, **126**, 696-697.

13 F. Hapiot, S. Tilloy, and E. Monflier. *Chem. Rev.*, 2006, **106**, 767-781.

14 W. Ciesielski and T. Girek. *J. Incl. Phenom. Macrocycl. Chem.*, 2011, **69**, 461-467.

15 B. Kaboudin, Y. Abedi and T. Yokomatsu. *Org. Biomol. Chem.*, 2012, **10**, 4543-4548.

16 G. Maccarrone, E. Rizzarelli and G. Vecchio. *Polyhedron*, 2002, **21**, 1531-1536.

17 D. Armspach, D. Matt, L. Poorters, R. Gramage-Doria, P. Jones and L. Toupet. *Polyhedron*, 2011, **30**, 573-578.

18 Y. Koito, K. Yamada and S. Ando. *J. Incl. Phenom. Macrocycl. Chem.*, 2012, **76**, 143-150.

19 D. Prochowicz, A. Kornowicz, I. Justyniak and J. Lewínski. *Coord. Chem. Rev.*, 2016, **306**, 331-345.

20 E. Norkus. *J. Incl. Phenom. Macrocycl. Chem.*, 2009, **65**, 237-248.

21 L.X. Song, J. Yang; L. Bai; F. Yun; J. Chen and M. Wang. *Inorg. Chem.*, 2011, **50**, 1682-1688.

22 Y. Guo, J. Li, F. Zhao, G. Lan, L. Li, Y. Liu, Y. Si, Y. Jiang, B. Yang and R. Yang. *RSC Adv.*, 2016, **6**, 7950-7954.

23 L.I. Rossi and R. Hoyos de Rossi. *J. Supramol. Chem.*, 2002, **2**, 509-514.

24 C. Kinen, L.I Rossi and R. Hoyos de Rossi. *Appl. Catal. A: Gen.*, 2006, **312**, 120-124.

25 L.I. Rossi and M.I. Velasco. *Pure Appl. Chem.*, 2012, **84**, 819-826.

26 S. Divakar. *J. Incl. Phenom. Mol. Recogn. Chem.*, 1994, **17**, 119-125.

27 B. Gyurcsik and L. Nagy. *Coord. Chem. Rev.*, 2000, **203**, 81-149.

28 H-J. Schneider, F. Hacket, V. Rüdiger and H. Ikeda. *Chem. Rev.*, 1998, **98**, 1755-1786.

29 A. Synytsya, M. Urbanová, V. Setnicka, M. Tkadlecová, J. Havlícek, I. Raich, P. Matejka, A. Synytsya, J. Copíková and K. Volka. *Carbohydr. Res.*, 2004, **339**, 2391-2405.

30 R.M. Gschwind. *Chem. Rev.*, 2008, **108**, 3029-3053.

31 W. Ciesielski and P. Tomasik, *J. Inorg. Biochem.*, 2004, **98**, 2039-51.

32 I. Villaescusa, N. Fiol, F. Cristiani, C. Floris, S. Lai and V. M. Nurchi, *Polyhedron*, 2002, **21**, 1363-1367.

View Article Online
DOI: 10.1039/C6DT01468B

33 L.H. Zhu, L.X. Song, X.Q. Guo and Z. Dang. *Thermochim. Acta*, 2010, **507-508**, 77-83.

34 P. Kubelka and F. Munk. *Z. Techn. Phys.*, 1931, **12**, 593-601.

35 CIE 15:2004. Colorimetry. 3th Ed. Commission Internationale de l'Eclairage, CIE.Technical Report.Publication 15:2004, ISBN 3-901-906-33-9.

36 O. Egyed. *Vib.Spectrosc.*, 1990, **1**, 225-227.

37 L.X. Song and Z. Dang. *J. Phys. Chem. B*, 2009, **113**, 4998-5000.

38 A. Magyar, Z. Szendi, J.T. Kiss and I. Pálinkó. *Theochem.*, 2003, **666-667**, 163-168.

39 J. Ferguson. *J. Chem. Phys.*, 1964, **40**, 3406-3410.

40 H. Ohtaki. *Pure Appl. Chem.*, 1987, **59**, 1143-1150.

41 A.S. Mereshchenko, P.K. Olshin, K.E. Karabaeva, M.S. Panov, R.M. Wilson, V.A. Kochemirovsky, M.Y. Skripkin, Y.S. Tveryanovich and A.N. Tarnovsky. *J. Phys. Chem. B*, 2015, **119**, 8754-8763.

42 F. Giordano, C. Novak, L. Caro and J.R. Moyano. *Thermochim. Acta*, 2001, **380**, 123-151.

43 A. Marini, V. Berbenni, G. Bruni, F. Giordano and M. Villa. *Thermochim. Acta*, 1996, **279**, 27-33.

44 R. Rodico Trinquinato, E.M. Pereira, M. Franco, M. Tavares and M.A. da Costa Ferreira. *Carbohyd. Res.*, 1999, **315**, 319-329.

45 L.I. Rossi and S.E. Martín. *Appl. Catal. A: Gral.*, 2003, **250**, 271-278.

46 M. Das and S. A. Shivashankar. *Appl. Organometal. Chem.*, 2007, **21**, 15-25.

47 N. D. Papadopoulos, H. S. Karayianni, P. E. Tsakiridis, M. Perraki, E. Sarantopoulou and E. Hristoforoua. *J. Electrochem. Soc.*, 2011, **158 (1)**, P5-P13.

48 A.W. Coats and J.P. Redfern. *Nature*, 1964, **20**, 68-69.

49 Y. Tonbul and K. Yurdakoç. *Turk. J. Chem.*, 2001, **25**, 333-339.

50 Y. Sarikaya, M. Önal, B. Baran and T. Alemdaroglu. *Clay and Clay Minerals*, 2000, **48**, 557-562.

51 S. Maitra, S. Mukherjee, N. Saha and J. Pramanik. *Ceramica*, 2007, **53**, 284-287.

52 M.M. Omar and G.G. Mohamed. *Spectrochim. Acta Part A*, 2005, **61**, 929-936.

View Article Online
DOI: 10.1039/C6DT01468B

53 The value of $\left(1-\frac{2RT}{E^*}\right)$ is approximately one (see ref. 47) and it is assumed first order reaction.

54 Y. Bai, J. Wang, M. Bashari, X. Hu, T. Feng, X. Xu, Z. Jin and Y. Tian. *Thermochim. Acta*, 2012, **541**, 62-69.

55 M.V. Rekharsky and Y. Inoue. *Chem. Rev.*, 1998, **98**, 1875-1917.

56 E.I. Solomon, D.E. Heppner, E.M. Johnston, J.W. Ginsbach, J.Cirera, M.Qayyum, M.T. Kieber-Emmons, C.H. Kjaergaard, R.G. Hadt and L.Tian. *Chem. Rev.*, 2014, **114**, 3659-3853.

57 B.J. Hathaway. *Coord. Chem. Rev.*, 1983, **52**, 87-169.

58 L.R. Falvello. *J. Chem. Soc. Dalton Trans.*, 1997, 4463-4476.

59 A.D. Shukla, H.C. Bajaj and A. Das. *Angew. Chem. Inter. Ed. Eng.*, 2001,**40**, 446-448.

60 T. Ishii, S. Tsuboi, G. Sakane, M. Yamashita and B.K. Breedlove. *Dalton Transaction*, 2009, 680-687.

61 M. Sánchez-Marañón, J.M. Martín-García and R. Delgado. *Geoderma*, 2011, **162**, 86-95.

62 G.R. Guzman, S.H. Hernandez, A. Ortiz, A.L.U. Dorantes, U.H. Hernandez and E.R. Mora. *Innov. Food Sci. Emerg. Techn.*, 2002, **3**, 47-53.

63 P.B. Merkel and C.M. Breeding. *Gems Gemology*, 2009, 112-119.

64 O. Opuchovic, G. Kreiza, J. Senvaitiene, K. Kazlauskas, A. Beganskiene and A. Kareiva. *Dyes Pigments*, 2015, **118**, 176-182.

65 J. Ortuño, R. Serrano, M.J. Jordán and S. Bañón. *Food Chem.*, 2016, **190**, 1056-1063.

66 F.J. Rodríguez-Pulido, R. Ferrer-Gallego, M.L. González-Mireta, J.C. Rivas-Gonzalo, M.T. Escribano-Bailón and F.J. Heredia. *Anal. Chim. Acta*, 2012, **732**, 78-82.

67 V. Sant'Anna, P.D. Gurak, L.D. Ferreira Marczak and I.C. Tessaro. *Dyes Pigments*, 2013, **98**, 601-608.

68 B.J. Hathaway. *Coord. Chem. Rev.*, 1981, **35**, 211-252.

69 A. Winter, K. Thiel, A. Zabel, T. Klamroth, A. Pöppl, A. Kelling, U. Schilde, A. Taubert and P. Strauch. *New J. Chem*., 2014, **38**, 1019-1030.

70 B.J. Hathaway and D.E. Billing. Coord. Chem. Rev. 1970, **5**, 143-207.

71 B.A. Goodman and J.B. Raynor. *Adv. Inorg. Chem. Radiochem.* 1970, **13**, 135-362.

View Article Online
DOI: 10.1039/C6DT01468B

72 J. Peisach and W.E. Blumberg, *Arch. Biochem. Biophys.* 1974, **165**, 691-708.

73 H. Langfelderov, D. Mala and P. Ger. *J. Thermal Anal.*, 1991, **37**, 2335-2346.

74 B. Małecka, R. Gajerski, A. Małecki, M. Wierzbicka and P. Olszewski. *Thermochim. Acta*, 2003, **404**, 125-132.

View Article Online
DOI: 10.1039/C6DT01468B

Graphical Synopsis

Structure characterization of non-crystalline complexes of copper salts with native cyclodextrins

Manuel I. Velasco,[a] Claudio R. Krapacher,[a] Rita Hoyos de Rossi,[a] Laura I. Rossi*.[a]

[a] Instituto de Investigaciones en Físico Química de Córdoba (INFIQC) - CONICET, Departamento de Química Orgánica, Facultad de Ciencias Químicas, Universidad Nacional de Córdoba, Ciudad Universitaria. X5000HUA Córdoba, Argentina.

e-mail: lauraros@fcq.unc.edu.ar

The characterization of non crystalline complexes is very difficult when techniques like X Ray diffraction or NMR are not available. We propose a simple procedure to characterize the physicochemical properties of amorphous new coordination compounds between cyclodextrins (CD) and Cu^{2+} salts, by means of the integration of the information provided by several techniques including elemental analysis, flame atomic absorption, TGA, FT-IR, EPR, UV-Vis Diffuse Reflectance and colorimetry. We also analyzed enthalpy-entropy compensation and isokinetic effect.

View Article Online
DOI: 10.1039/C6DT01468B

Graphical Abstract

Structure characterization of non-crystalline complexes of copper salts with native cyclodextrins

Manuel I. Velasco, Claudio R. Krapacher, Rita Hoyos de Rossi, Laura I. Rossi*.

Instituto de Investigaciones en Físico Química de Córdoba (INFIQC) - CONICET,
Departamento de Química Orgánica, Facultad de Ciencias Químicas, Universidad Nacional de Córdoba, Ciudad Universitaria. X5000HUA Córdoba, Argentina.

e-mail: lauraros@fcq.unc.edu.ar